2011

Charge Saturation and Neutral Substitutions in Halomethanes and Their Group 14 Analogues

Bernard K. Wittmaack

Chad Crigger

Matthew Guarino

Kelling J. Donald
University of Richmond, kdonald@richmond.edu

Recommended Citation

Wittmaack, Bernard K., Chad Crigger, Matthew Guarino, and Kelling J. Donald. "Charge Saturation and Neutral Substitutions in Halomethanes and Their Group 14 Analogues." *Journal of Physical Chemistry* 115, no. 31 (2011): 8743-8753. doi:10.1021/jp204316h.

THE JOURNAL OF
PHYSICAL CHEMISTRY A

ARTICLE

pubs.acs.org/JPCA

Charge Saturation and Neutral Substitutions in Halomethanes and Their Group 14 Analogues

Bernard K. Wittmaack, Chad Crigger, Matthew Guarino, and Kelling J. Donald*

Department of Chemistry, Gottwald Center for the Sciences, University of Richmond, Richmond, Virginia 23173, United States

S *Supporting Information*

ABSTRACT: A computational analysis of the charge distribution in halomethanes and their heavy analogues ($MH_{4-n}X_n$: M = C, Si, Ge, Sn, Pb; X = F, Cl, Br, I) as a function of n uncovers a previously unidentified saturation limit for fluorides when $M \neq C$. We examine the electron densities obtained at the CCSD, MP2(full), B3PW91, and HF levels of theory for 80 molecules for four different basis sets. A previously observed substituent independent charge at F in fluoromethanes is shown to be a move toward saturation that is restricted by the low polarizability of C. This limitation fades into irrelevance for the more polarizable M central atoms such that a genuine F saturation is realized in those cases. A conceptual model leads to a function of the form $[q_{M(n')} - q_{M(n)}] = a[\chi_{A'} - \chi_A] + b$ that links the electronegativities (χ) of incoming and leaving atoms (e.g., A′ = X and A = H for the halogenation of $MH_{4-n}X_n$) and the associated charge shift at M. We show that the phenomenon in which the charge at the central atom, q_M, is itself independent of n (e.g., at carbon in $CH_{4-n}Br_n$) is best described as an "M-neutral substitution"—not saturation. Implications of the observed X saturation and M-neutral substitutions for larger organic and inorganic halogenated molecules and polymeric materials are identified.

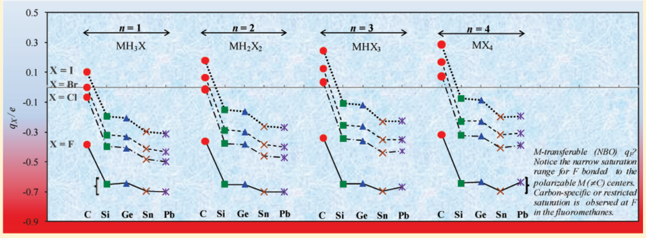

M-transferable (NBO) q_F? Notice the narrow saturation range for F bonded to the polarizable M (≠C) centers. Carbon-specific or restricted saturation is observed at F in the fluoromethanes.

1. INTRODUCTION

The usefulness of point charges in chemical pedagogy and in the analyses of reactivity and bonding in molecules is undeniable.[1] This is so despite contentions about the reliability of the various strategies used to obtain point charges and the meaning of the resulting charges.[2] Early semiempirical electrostatic (point charge) models such as the Rittner[3] and the bond-charge[4] models have found success as descriptors, for example, of the qualitative variations in dipole moments and force constants in diatomic molecules. They tend to be unreliable as quantitative tools for larger molecules[5−8] and especially so for systems in which relativistic effects are important.[8] Nonetheless, the continued successes of point charge models for small molecules,[9] and the use of charges in force fields (especially important for large organic and biologically relevant molecules),[10] have guaranteed a space in the chemical discourse for atomic charges. The ability to bridge quantum mechanical calculations and qualitative understanding by reference to point charge representations, and the interconnections between atomic point charges (q) and other concepts such as electronegativity (χ), hybridization, and bond order have definitely helped as well.

In tacit acknowledgment of the utility of point charges in chemistry, a number of different strategies for obtaining atomic charges[11] are routinely implemented in modern computational packages, and the data they provide are commonly referenced in rationalizing electronic and geometrical phenomena in molecules.

In two earlier contributions,[12,13] Donald et al. investigated the evolution of the charge distribution in the halomethanes and their Si, and Ge analogues ($MH_{4-n}X_n$: M = C, Si, Ge; X = F, Cl, Br) as a function of the number of halides, n. We use the term "evolution" because we are concerned primarily with the direction and the extent of the *charge shifts* (not the magnitudes of the charges per se) that are induced at the M and X sites by successive geminal halogen substitutions.

Of particular relevance to this work is our brief discussion in ref 13 of the so-called "saturation effect"[14] at M in certain $MH_{4-n}X_n$ molecules: that is, the observation that the charge at the central atom, q_M, is practically independent of n such that $\Delta q_{M(n \rightarrow n')} = q_M(MH_{4-n'}X_{n'}) - q_M(MH_{4-n}X_n)$ is very close to zero for any change in n. We showed in ref 13 that this effect (identified previously by Wiberg and Rablen for q_C in $CH_{4-n}Cl_n$)[14] is observed in the chloro- and bromosilanes, and germanes as well, and is, therefore, not unique to organic systems. And, with reference to a point charge description of the $MH_{4-n}X_n$ molecules, we posited a simple model based on electronegativities to account for the apparent M-saturation in the C, Si, and Ge systems.[13]

In this contribution, we derive a completely general electronegativity-difference function (which links $\Delta q_{M(n \rightarrow n')}$ and $\chi_X - \chi_H$), and we extend our analysis to include the computationally more demanding halostannane and haloplumbane systems. The iodides, which were neglected in refs 12 and 13, are taken into account in this work as well. The complete series of molecules ($MH_{4-n}X_n$: n = 1−4; M = C, Si, Ge, Sn, Pb; X = F, Cl, Br, I) have been

Received: May 9, 2011
Revised: June 7, 2011
Published: June 09, 2011

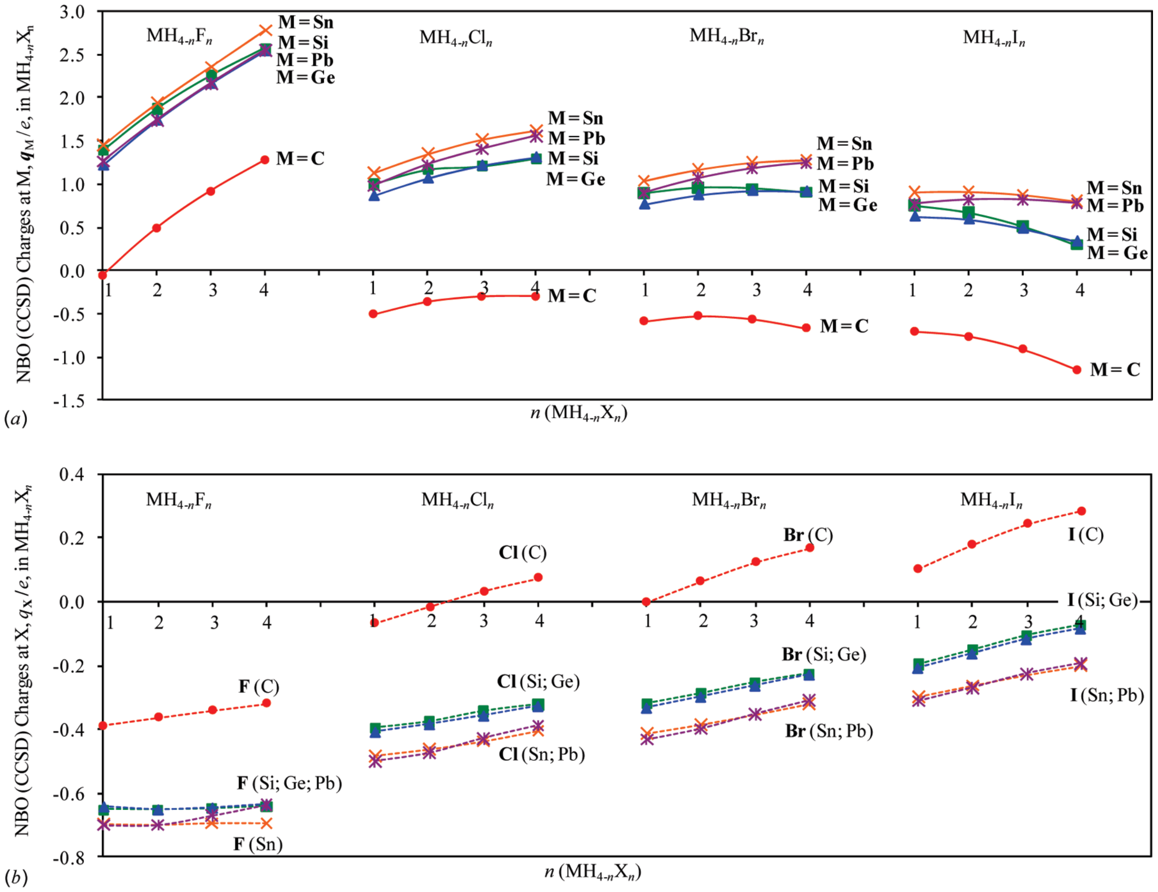

Figure 1. (a) NBO point charges obtained at the CCSD level of theory for the central atoms, q_M. (b) NBO point charges obtained at the CCSD level of theory for the halides, q_X. The q_M and q_X data plotted in Figure 1a,b and the corresponding q_H values are listed in the Supporting Information. For the elements preceding Sn in the periodic table, the aug-cc-pVTZ basis sets were used. For the heavier elements, the basis sets and ECPs are given in the Computational Methods.

(re)optimized in our group recently at the MP2(full) level of theory as part of a larger study of halogen bonding.[15] In this paper, we investigate the substituent dependence of the charge distribution in the $MH_{4-n}X_n$ systems. We uncover an explanation for the apparent "saturation effect" at M, and propose an ansatz for predicting the n dependence of the charge at M, $q_M(n)$, in the simple organic compounds (for M = C), and in their Si, Ge, Sn, and Pb counterparts.

The saturation concept has been used to account for the insensitivity of the charge density at certain terminal X atoms to geminal halogenations as well.[11,14,16] We locate in this work a previously unidentified charge saturation phenomenon at F atoms (q_F) that is achieved only when $M \neq C$ (compared to far smaller but also quite consistent charge transfer from C to F in $CH_{4-n}F_n$). We show that an apparent M-saturation in some of the $MH_{4-n}X_n$ series (the n-independence of q_M in some cases when X = Cl, Br, or I) is specious and is best described as a set of M-neutral substitutions: instances in which the electron withdrawing power of X is such that increasing n in $MH_{4-n}X_n$ has little or no effect on q_M. For the terminal X atoms in the $MH_{4-n}X_n$ molecules, however, the n-independence of the q_F (for $M \neq C$) is a genuine manifestation of the saturation phenomenon. The observed fluorine saturation (an n-independent charge distribution at F in $MH_{4-n}F_n$) persists for M = Si, Ge, Sn, and Pb.

Our observation that q_F for $M \neq C$ is more negative than q_F in the halomethanes has, we consider, potentially significant physical and experimentally testable implications beyond the fundamental analysis in this report. An extension of our current results to polymeric materials suggests that the hydrophobicity and other properties of organic fluoropolymers (e.g., Teflon $-(CF_2)_n-$) that depend on electrostatics, may be significantly modified when $M \neq C$, because q_F is much more negative in those cases.

An important decision that one has to make in a study such as this is to select specific population analysis strategies to consider. There are several, each with its particular set of advantages.[11,14] As our sources for the charge separation in the $MH_{4-n}X_n$ molecules, however, we rely on the well-studied natural bond orbital (NBO) analysis,[17] supplemented by references to the atoms-in-molecules (AIM)[18] and atomic polar tensor (APT)[19] methods. A justification of our selection of the NBO method as our primary analytical tool is provided in the Computational Methods. The trends observed in the NBO data in this work are comparable in general to those obtained from the AIM and APT values as well.

2. COMPUTATIONAL METHODS

The geometrical data reported in this work have been obtained at the Møller–Plesset (MP2(full)) level of theory.[20]

The 6-311+G* basis sets[21] have been employed for H and the lighter elements in both groups 14 and 17: M = C, Si, Ge and X = F, Cl, Br. For the computationally more demanding cases, M = Sn, Pb and X = I, we used scalar-relativistic energy-consistent small core Dirac−Fock (MDF) effective-core pseudopotentials (ECPs): 28*e* cores for Sn and I, a 60*e* core for Pb (without the spin−orbit potential but including the scalar relativistic effects), and the corresponding basis sets.[22a−e] In the single instance in which it is mentioned in this report, a 60*e* core MDF ECP is used for At.[22f] To test the dependence of the population analyses on the choice of model chemistry, we started with the optimized geometries obtained at the MP2(full) level mentioned above and computed the NBO point charges at sixteen different levels: combining the 6-311+G*,[21] 6-311++G**,[23] cc-pVTZ,[24] and aug-cc-pVTZ[25] basis sets with the HF,[26] B3PW91,[27] MP2(full),[20] and CCSD[28] methods for all 80 of the $MH_{4-n}X_n$ molecules. For the elements heavier than Br, we used the pseudopotentials and basis sets mentioned above in each case. So, only one set of values was obtained for SnI_4 and PbI_4; these values are used in all cases below where we refer to those two molecules. For comparison with the trend in the NBO data,[17] the AIM[18] and APT[19] population analyses have also been performed at the MP2(full) computational level mentioned above at which the structures were optimized. All ab initio calculations were performed using the Gaussian 03 suite of programs.[29] We focus on the NBO analysis over the other population analysis methods because it is arguably the most common strategy in the current literature for obtaining atomic charges and is implemented in Gaussian 03 for all the atoms considered in this work. The AIM method is unavailable for systems whose cores are described by pseudopotentials.

3. RESULTS AND DISCUSSION

3.1. Charge Distribution in Halomethanes and Their Heavy Analogues. A set of the NBO charges obtained at the CCSD level for M in the $MH_{4-n}X_n$ systems (M = C, Si, Ge, Sn, Pb; X = F, Cl, Br, I) are plotted in Figure 1a. The corresponding q_X charges are shown in Figure 1b, but we will focus on the M centers for now. Almost identical plots have been obtained using the HF, B3PW91, and MP2 model chemistries (see the Supporting Information).[30] This work focuses primarily on the $MH_{4-n}X_n$ systems with $1 \leq n \leq 4$. Nonetheless, we have included in the Supporting Information an extended version of Figure 1a that features the q_M values for the MH_4 ($n = 0$) molecules as well.

The first question we ask is that of the influence of halogenation on the electron density at central atoms. Figure 1a suggests that *halogen substitution does not always make the central atom more positive*. The charge at M, q_M, definitely becomes more positive when X is fluorine (on the left in Figure 1a). Going across Figure 1a (from X = Cl to X = I), however, the situation is reversed gradually (as X becomes less electronegative going from X = Cl to X = Br and I) such that increasing *n* when X = I always makes M more negative. This is readily seen by comparing the slopes of the fluoride and the iodide curves in Figure 1a. For most of the M centers, the chlorides and bromides are intermediate cases where the charge transferred to or from the M center as *n* changes is small. For the chlorides, the $\Delta q_{M(n\to n')}$ values are typically small and positive. They are even smaller for the bromides and are actually very slightly negative for the $\Delta q_{C(3\to 4)}$ case. Indeed, for the bromomethanes the Δq_C values for X = Br are so small (consequences of a competition between geometrical and electronic factors examined in ref 13) that the $CH_{4-n}Br_n$ curve in Figure 1a is essentially flat.

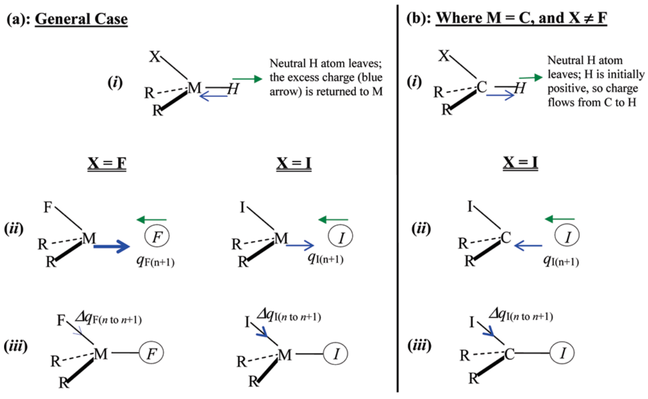

Figure 2. (a) Stepwise summary of the evolution in q_M and q_X in the $MH_{4-n}X_n$ molecules going from *n* to $n' = n + 1$ for X = F and X = I (where R is X or H, depending on the value of *n*). The blue arrows represent the net flow of electrons and the green arrows show the incoming or outgoing atom at each stage. (i) H atom elimination (via homolytic bond cleavage). The blue arrow indicates the flow of electrons to M (because H was negatively charged). (ii) Rehybridization at M and bonding to the incoming (circled) X atom. (iii) Relaxation of the other (X or H) sites, with an inductive charge shift toward M. (b) Exceptional case for the less electronegative X atoms (represented by I) when M = C. In those cases, q_H is typically positive, so electron density is shifted from C to H at stage i and X donates electron density to M at stages ii and iii.

Interestingly, this move from a positive $\Delta q_{M(1\to 4)}$ for X = F to a negative $\Delta q_{M(1\to 4)}$ value for X = I is observed for all M in Figure 1a, with a flat line ($\Delta q_{M(1\to 4)} \approx 0.0$) occurring for a certain X along the way. For the M = C case (the red lines in Figure 1a), we find that $\Delta q_{C(1\to 4)} = q_C(CX_4) - q_C(CH_3X) = +1.33e$ for X = F, and $+0.22e$, $-0.08e$, and $-0.44e$ for X = Cl, Br, and I, respectively. This quantifies for us just how dramatically Δq_M varies and unmasks the bromomethane curve in Figure 1a as a flat waypoint at which q_C is roughly independent of *n*.

The cases for X = Cl, and for X = Br in particular (in which $|\Delta q_{C(1\to 4)}|$ is a mere 0.08*e*), illustrate what has been described as a *saturation* at the carbon center in these compounds. This phenomenon was identified in the chloro- and cyanomethanes by Wiberg and Rablen in 1993.[14] In that work, the stability of CF_4 (relative to CCl_4, for example) is explained by the absence of a saturation effect in $CH_{4-n}F_n$. The continuous increase in q_C (see the $CH_{4-n}F_n$ curve in Figure 1a) and the constant q_F (see Figure 1b) as *n* increases causes the C---F Coulomb attraction in $CH_{4-n}F_n$ to intensify with each increase in *n*, which culminates at CF_4. Wiberg and Rablen showed that a similar electrostatic stabilization is not observed when X = Cl because q_C hardly changes with *n* in that case (i.e., CF_4 is more stable because of the evident saturation at C in CCl_4).

3.2. Δq_M: High at F; Low or Negative at I. The apparent cases of saturation at C in $CH_{4-n}Cl_n$ and $CH_{4-n}Br_n$ in Figure 1a seem, however, to be simply waypoints in a progression from a positive Δq_C at X = F to a negative Δq_C at X = I. As far as the charge density at carbon is concerned, Br mimics H such that $\Delta q_C \approx 0$, but this insensitivity of q_C to the Br substitution does not signal the attainment of any special saturation at C in $CH_{4-n}Br_n$ per se. The charge shift, Δq_C, is roughly zero at X = Br but becomes quite negative for X = I ($-0.44e$) and, we find, is even a bit more negative at X = At ($-0.49e$).

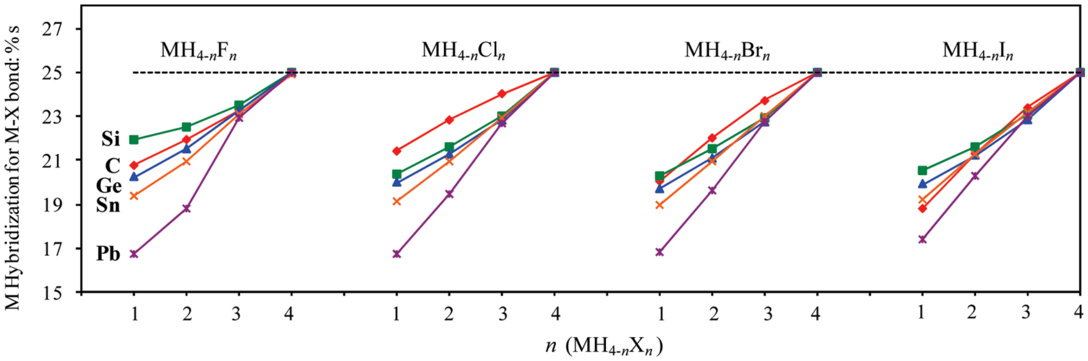

Figure 3. % s composition at M in the M—X bonds of the $MH_{4-n}X_n$ molecule. These NBO analysis data were obtained for structures optimized at the MP2(full) level of theory using the 6-311+G* basis set for atoms above Sn in the periodic table, and the basis sets and ECPs mentioned in the Computational Methods for all the other elements.

Table 1. Pauling and Absolute (Mulliken) Ground State Electronegativities for H, and the Halides and the Valence State (100% p) Orbital Values for the Halides (χ^P, $\chi^{M(GS)}$, and $\chi^{M(VS)}$(p))[a]

	electronegativities		
	χ^P	$\chi^{M(GS)}$/eV	$\chi^{M(VS)}$(p)/eV
H	2.2	7.18	
F	3.98	10.41	12.20
Cl	3.16	8.30	9.35
Br	2.96	7.59	8.83
I	2.66	6.76	7.96

[a] The Pauling and ground state absolute electronegativities are from ref 34. The valence state electronegativities for the X atoms are from ref 32.

Now, we have used the M = C case to motivate the discussion, but the trend toward a negative Δq_M as X gets larger is not unique to the carbon compounds. The curves in Figure 1a for M = Si, Ge, Sn, and Pb mirror the C cases. The $\Delta q_M \approx 0$ waypoints (where the curves in Figure 1a are nearly horizontal) occur at X = Br and even X = I for the larger M atoms, but the tendency toward negative Δq_M is quite obvious. The AIM data in the Supporting Information show the identical trends; for the APT method Δq_M decreases as well, although it never becomes negative.

3.3. Modeling Substitution-Induced Charges Transfers in $MH_{4-n}X_n$ Systems. We wanted to rationalize and unify our observations on the n-dependent charge distribution in the $MH_{4-n}X_n$ compounds, in particular, the apparent saturation and noticeable increase in the negative character at M as X gets larger. So, we formulated a simple scheme for the changes in the charge distribution in the molecules during halogen substitution. The illustrations in Figure 2 are for the cases where X = F and X = I (the two extremes in Figure 1a,b). *Note that these schemes are not reaction mechanisms.* They are summaries of how the charges at X and M evolve as n increases, regardless of the mechanism by which the substitution occurs.

The first stage in Figure 2, (i), is the removal of a H atom from the $MH_{4-n}X_n$ molecule. We assume at this stage that this H elimination affects the charge density at the M center only, and we freeze the three remaining (H or X) substituents. In step ii, the M atom rehybridizes as it bonds to the new (incoming) X substituent.[31] As we show in Figure 3, *the s compositions of the M hybrid orbitals in the M—X bond always increase as n increases.* Eventually, at $n = 4$ (in the tetrahedral MX_4), the hybrid orbitals attain the expected ~25% s (sp^3) orbital composition. This increase in the % s composition is in accordance with our observation that for the less electronegative X atoms (Br and I) M gets more negative going from $n = 1$ to $n = 4$. It is well-known that an increase in the valence s contribution increases the orbital electronegativity.[32]

The significant differences in the charge transferred to the incoming X atom as X gets less electronegative going down group 17 from F to I is indicated in Figure 2a by the bold (and thin) blue arrows at stage ii for X = F (and X = I). We require at stage ii (however, pre-emptively) that the charge transferred between M and this incoming X substituent be exactly what it should be in the final relaxed product. Put another way, the charge at this new X site is already $q_{X(n+1)}$; it will require no adjustment after we unfreeze the other three substituents.

Now, if the effective electronegativity of X is sufficiently large compared to that of the H atom it replaced (i.e., if $\chi_X \gg \chi_H$), the charge shift from M into the bonding region at stage ii will be significantly more than the charge returned to M at stage i. So, the M center will be more electrophilic after stage ii than it was before the H elimination. At stage iii, therefore, when we unfreeze the other three atoms, the geometrical relaxation of the molecule[31] will be accompanied by *a net flow of electron density* ($\Delta q_{X(n\rightarrow n+1)}$) *(however incremental) from those three terminal atoms toward M.* It is not surprising, therefore, that for all the halides, q_X becomes slightly more positive with each increase in n (Figure 1b). *So, rehybridizing and bonding to the incoming X substituent makes M more electron withdrawing such that all the X sites become a bit more positive.*[33]

However, the more electronegative the initially frozen substituents are the smaller the transfer at stage iii will be. This explains the insensitivity of the fluorides in Figure 1b to n, which we indicate in Figure 2 with the small arrowhead for X = F on the bond at stage iii. The change in q_M is significant for each F substitution, but the fluorides are sufficiently electronegative to remain almost unaffected. For the heavier halides, however, the charge transfers from X to M (for any change in n) is somewhat more significant, as is evident in the slightly larger slopes for the X ≠ F lines in Figure 1b compared to the F case. By the scheme in Figure 2, a neutral substitution (the perceived M-saturation) occurs when the charge transfer in one direction at stage i happens to be just offset by the net charge transfer in the opposite direction at stages ii and iii.

3.4. Quantifying Charge Transfers. As a first approximation, Donald et al. suggested in ref 13 that the perceived saturation at

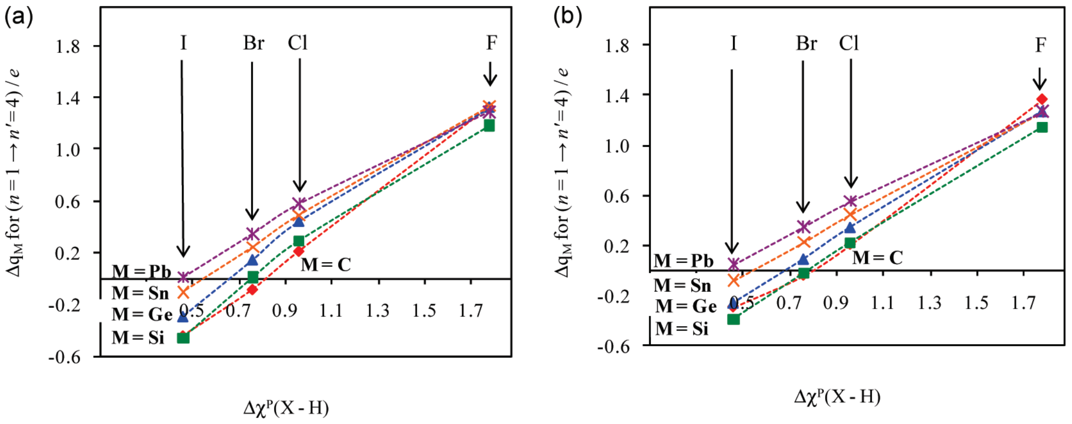

Figure 4. (a) NBO (CCSD) $\Delta q_{M(n=1\rightarrow n'=4)}$ vs$\Delta\chi^P{}_{(X-H)}$ for the $MH_{4-n}X_n$ molecules. For the atoms lighter than Sn, the aug-cc-pVTZ basis sets were used. The linear equation and correlation coefficient for the five data sets identified by the colored linkers are listed in Table 2. (b) NBO (MP2) $\Delta q_{M(n=1\rightarrow n'=4)}$ vs$\Delta\chi^P{}_{(X-H)}$ for the $MH_{4-n}X_n$ molecules. For the atoms lighter than Sn, the 6-311++G** basis sets were used. The linear equation and correlation coefficient for the five data sets identified by the colored linkers are listed in Table 2.

M in the $CH_{4-n}X_n$, $SiH_{4-n}X_n$, and $GeH_{4-n}X_n$ molecules (when $\Delta q_M \approx 0$, for X = Cl or Br) may be explained qualitatively by the difference in the electronegativities of H and the X substituents;[32,34] that is, $\Delta\chi_{(X-H)}$ ($=\chi_X - \chi_H$), going down group 17 from X = F to X = I.

They posited that, for a given change in n (from some n to n') in $MH_{4-n}X_n$, the corresponding change in q_M ($\Delta q_{M(n\rightarrow n')}$) should vary directly with $\Delta\chi_{(X-H)}$. So, since we know (see Table 1) that $\Delta\chi_{(X-H)}$ (for X = F, Cl, Br, and I) varies as

$$\Delta\chi_{(F-H)} \gg \Delta\chi_{(Cl-H)} > \Delta\chi_{(Br-H)} > \Delta\chi_{(I-H)} \qquad (1)$$

we expect that

$$\Delta q_M(X = F) \gg \Delta q_M(X = Cl) > \Delta q_M(X = Br) > \Delta q_M(X = I) \quad (\text{for any change } n \rightarrow n') \qquad (2)$$

This basic inference is confirmed in the present work for the complete series of group 14 $MH_{4-n}X_n$ compounds, (including $SnH_{4-n}X_n$, $PbH_{4-n}X_n$, and the iodides), which has not been considered before. Moreover, we derive a simple mathematical relationship between expressions 1 and 2 that applies with equal reliability to all M centers.

3.4.1. A Heuristic Justification. We wanted to understand better the exact relationship between $\Delta q_{M(n\rightarrow n')}$ and $\Delta\chi_{(X-H)}$. The two parameters are implicitly linked by expressions 1 and 2, and we converge on a more formal relationship by the following deliberation. Let us assume that, for the general theoretical reactions, (i) A + $^{\bullet}MH_{3-n}X_n$ (i.e., atom A bonding to a substituted methyl radical), and (ii) A′ + $^{\bullet}MH_{3-n}X_n$, the charge transfers between M and A or between M and A′ are proportional to $\chi_A - \chi_M$ and $\chi_{A'} - \chi_M$, respectively, where, χ_M is the electronegativity at M in the $^{\bullet}MH_{3-n}X_n$ radical. Then, where A = H and A′ = X we can write

$$q_{M(n)} - q_{M,\text{radical}} \propto \chi_H - \chi_M \quad \text{and}$$
$$q_{M(n')} - q_{M,\text{radical}} \propto \chi_X - \chi_M \qquad (3)$$

which implies by subtraction of the two equations that $\Delta q_{M(n\rightarrow n')} = a(\Delta\chi_{(X-H)})$ or, more generally,

$$\Delta q_{M(n\rightarrow n')} = a(\Delta\chi_{(X-H)}) + b \qquad (4)$$

where a and b are constants, and ideally, $b = 0$.

So, for a set of X atoms that bond in an identical fashion to M (such as the set of halide substituents, X, which are all univalent and valence-isoelectronic) we expect that $\Delta q_{M(n\rightarrow n')}$ vs $\Delta\chi_{(X-H)}$ will give a straight line for the (unfortunately only four) data points: X = F, Cl, Br, and I.

To test eq 4, we plotted, for all five M atoms, $\Delta q_{M(n\rightarrow n')}$ as a function of $\Delta\chi^P{}_{(X-H)}$ (see χ data in Table 1) for X = F, Cl, Br, and I for the different (HF, B3PW91, MP2, and CCSD) model chemistries considered in this work. The sample MP2 and CCSD plots shown in Figure 4a,b are typical of the relationships that we have found at the various computational levels (with additional plots included in Figure S.5 of the Supporting Information).

The data in Figure 4a,b (see also the series shown in the Supporting Information) reveal an extremely high linear correlation between ($\Delta q_{M(1\rightarrow 4)}$) and $\Delta\chi^P{}_{(X-H)}$ in all cases, in good agreement with eq 4. We have used colored connecting lines in Figure 4 for clarity to identify the various data sets (for M = C, Si, Ge, Sn, and Pb). The actual best fit lines are not shown, but we have provided in Table 2 the values of a and b and the corresponding coefficients of determination (R^2) for all cases.

The data shown in Figure 4 are all for the extreme case $\Delta q_{M(n=1\rightarrow n'=4)}$ where $\Delta n = 3$. That is, three H atoms in MH_3X have been replaced by three X atoms to give MX_4. However, as Table 2 confirms, similar high quality plots are obtained for Δn = 1 ($\Delta q_{M(n=1\rightarrow n'=2)}$) and Δn = 2 ($\Delta q_{M(n=1\rightarrow n'=3)}$) as well. So, the relationship in eq 4 holds, with $0.990 \le R^2 \le 1.000$, and can be used to monitor charge shifts at M for any change in n and the relevant $\Delta\chi_{(X-H)}$.

It is satisfying that this general linear relationship between Δq and $\Delta\chi$ is not specific to the Pauling electronegativities (Table 1) we used in obtaining the data in Table 2. The absolute (Mulliken) electronegativities for the halides vary linearly with the Pauling values and would give, therefore, similar results. Indeed, quite good results are obtained as well with the (100% p) valence state electronegativities obtained from Bratsch (Table 1).[32,35]

The Pauling electronegativity scale, which itself is obtained from a definition of $\Delta\chi_{(X-H)}$ in terms of bond dissociation energies,[36] is a convenient choice. That definition of $\Delta\chi$ together with eq 4 implies a direct relationship too between the charge shifts at the M centers when H is replaced by X (Δq_M), and the H—X bond dissociation energies.[37]

Table 2. Constants a, b, and Coefficients of Determination for the Equation $[q_{M(n')} - q_{M(n)}] = a[\chi_X - \chi_H] + b$, Which Describes (see Figure 4) the Computed (NBO) Charge Shifts at M in the $MH_{4-n}X_n$ Molecules Considered in This Work for Several Different Model Chemistries

		6-311+G*			6-311++G**			cc-pVTZ			aug-cc-pVTZ		
	Δn	a	b	R^2	a	b	R^2	a	b	R^2	a	b	R^2
						M = C							
HF	1	0.508	−0.334	0.996	0.508	−0.328	0.996	0.470	−0.264	1.000	0.496	−0.302	0.999
	2	0.982	−0.716	0.997	0.980	−0.706	0.996	0.900	−0.578	1.000	0.950	−0.656	1.000
	3	1.450	−1.144	0.997	1.389	−1.104	0.998	1.350	−0.997	0.999	1.407	−1.098	1.000
B3PW91	1	0.466	−0.282	0.994	0.466	−0.275	0.994	0.427	−0.213	0.998	0.450	−0.253	0.997
	2	0.893	−0.607	0.996	0.891	−0.595	0.996	0.825	−0.488	1.000	0.869	−0.566	0.999
	3	1.324	−0.989	0.995	1.326	−0.988	0.995	1.236	−0.859	0.999	1.289	−0.954	0.999
MP2	1	0.458	−0.272	0.991	0.455	−0.270	0.991	0.430	−0.225	0.999	0.454	−0.262	0.997
	2	0.873	−0.584	0.992	0.871	−0.587	0.992	0.821	−0.503	1.000	0.882	−0.599	0.998
	3	1.287	−0.948	0.991	1.288	−0.967	0.991	1.250	−0.891	0.999	1.314	−1.012	0.999
CCSD	1	0.467	−0.294	0.993	0.463	−0.292	0.993	0.439	−0.248	0.999	0.462	−0.284	0.998
	2	0.897	−0.632	0.994	0.894	−0.638	0.994	0.857	−0.559	1.000	0.904	−0.645	0.999
	3	1.329	−1.027	0.993	1.330	−1.050	0.993	1.284	−0.960	1.000	1.349	−1.080	0.999
						M = Si							
HF	1	0.433	−0.266	1.000	0.424	−0.262	1.000	0.409	−0.228	0.998	0.414	−0.248	0.989
	2	0.832	−0.560	0.999	0.829	−0.572	0.999	0.769	−0.458	0.991	0.798	−0.520	0.987
	3	1.211	−0.872	0.999	1.220	−0.909	0.999	1.139	−0.763	0.983	1.184	−0.854	0.982
B3PW91	1	0.428	−0.243	1.000	0.422	−0.247	1.000	0.397	−0.188	0.996	0.419	−0.230	0.997
	2	0.814	−0.514	1.000	0.808	−0.525	1.000	0.762	−0.429	0.995	0.803	−0.497	0.992
	3	1.188	−0.818	0.999	1.192	−0.848	0.999	1.103	−0.681	0.984	1.170	−0.799	0.988
MP2	1	0.405	−0.239	1.000	0.404	−0.262	1.000	0.383	−0.213	0.995	0.416	−0.257	0.995
	2	0.774	−0.510	1.000	0.781	−0.561	1.000	0.733	−0.468	0.988	0.813	−0.572	0.990
	3	1.135	−0.818	0.999	1.155	−0.902	1.000	1.086	−0.786	0.982	1.205	−0.939	0.987
CCSD	1	0.411	−0.237	1.000	0.408	−0.268	0.999	0.389	−0.217	0.995	0.421	−0.259	0.996
	2	0.785	−0.507	1.000	0.787	−0.570	1.000	0.744	−0.473	0.989	0.824	−0.594	0.998
	3	1.150	−0.814	1.000	1.163	−0.912	1.000	1.099	−0.789	0.983	1.215	−0.947	0.991
						M = Ge							
HF	1	0.426	−0.226	0.999	0.421	−0.235	1.000	0.405	−0.188	0.995	0.421	−0.225	0.999
	2	0.834	−0.491	0.999	0.828	−0.510	0.999	0.781	−0.406	0.995	0.816	−0.475	0.997
	3	1.233	−0.786	0.998	1.236	−0.827	0.998	1.142	−0.649	0.995	1.195	−0.737	0.992
B3PW91	1	0.408	−0.194	1.000	0.406	−0.207	1.000	0.372	−0.130	0.999	0.404	−0.181	0.994
	2	0.794	−0.430	1.000	0.794	−0.455	1.000	0.733	−0.326	0.998	0.783	−0.410	0.997
	3	1.171	−0.699	0.999	1.177	−0.739	0.999	1.076	−0.547	0.996	1.157	−0.681	0.995
MP2	1	0.400	−0.194	1.000	0.392	−0.209	1.000	0.371	−0.160	0.997	0.408	−0.204	0.997
	2	0.777	−0.433	1.000	0.775	−0.476	1.000	0.716	−0.360	0.994	0.799	−0.462	0.993
	3	1.150	−0.711	1.000	1.159	−0.786	1.000	1.058	−0.605	0.990	1.188	−0.770	0.992
CCSD	1	0.393	−0.190	1.000	0.389	−0.216	1.000	0.379	−0.169	0.997	0.414	−0.211	0.997
	2	0.765	−0.425	1.000	0.767	−0.486	1.000	0.731	−0.377	0.995	0.810	−0.473	0.993
	3	1.134	−0.701	1.000	1.148	−0.798	0.999	1.079	−0.626	0.991	1.202	−0.783	0.993
						M = Sn							
HF	1	0.368	−0.139	0.999	0.365	−0.151	0.999	0.361	−0.125	0.993	0.368	−0.147	0.999
	2	0.729	−0.322	0.998	0.730	−0.352	0.998	0.726	−0.320	0.994	0.740	−0.353	0.996
	3	1.081	−0.534	0.999	1.088	−0.577	0.999	1.074	−0.534	0.995	1.028	−0.536	0.992
B3PW91	1	0.356	−0.115	0.999	0.353	−0.128	1.000	0.346	−0.105	0.998	0.354	−0.121	0.999
	2	0.691	−0.264	0.999	0.691	−0.293	0.999	0.667	−0.239	0.998	0.696	−0.283	0.999
	3	1.023	−0.457	0.999	1.030	−0.499	0.999	0.983	−0.417	0.997	1.040	−0.491	0.998
MP2	1	0.353	−0.119	1.000	0.350	−0.143	1.000	0.341	−0.124	0.996	0.354	−0.141	0.996
	2	0.685	−0.277	1.000	0.684	−0.322	1.000	0.661	−0.284	0.994	0.693	−0.320	0.995
	3	1.013	−0.471	1.000	1.021	−0.543	1.000	0.977	−0.490	0.995	1.036	−0.550	0.997

Table 2. Continued

		6-311+G*			6-311++G**			cc-pVTZ			aug-cc-pVTZ		
	Δn	a	b	R^2	a	b	R^2	a	b	R^2	a	b	R^2
M = Sn													
CCSD	1	0.356	−0.116	1.000	0.353	−0.146	1.000	0.348	−0.131	0.996	0.359	−0.146	0.996
	2	0.693	−0.271	1.000	0.693	−0.328	1.000	0.677	−0.297	0.995	0.704	−0.329	0.995
	3	1.026	−0.468	1.000	1.035	−0.556	1.000	1.000	−0.508	0.996	1.083	−0.583	0.999
M = Pb													
HF	1	0.333	−0.074	0.997	0.328	−0.085	0.997	0.322	−0.059	0.996	0.327	−0.075	0.995
	2	0.672	−0.205	0.997	0.670	−0.229	0.997	0.653	−0.181	0.995	0.673	−0.220	0.995
	3	0.996	−0.363	0.997	1.003	−0.402	0.997	0.967	−0.331	0.993	1.015	−0.398	0.995
B3PW91	1	0.311	−0.049	0.998	0.307	−0.061	0.998	0.298	−0.036	0.995	0.311	−0.061	0.996
	2	0.620	−0.152	0.998	0.619	−0.177	0.998	0.590	−0.123	0.995	0.623	−0.175	0.996
	3	0.905	−0.280	0.997	0.911	−0.318	0.997	0.851	−0.229	0.992	0.915	−0.313	0.995
MP2	1	0.313	−0.048	0.999	0.309	−0.071	0.999	0.302	−0.053	0.991	0.305	−0.065	0.989
	2	0.621	−0.152	0.999	0.621	−0.198	0.999	0.600	−0.159	0.992	0.624	−0.192	0.991
	3	0.911	−0.286	0.998	0.919	−0.355	0.998	0.874	−0.298	0.991	0.934	−0.363	0.994
CCSD	1	0.317	−0.051	0.999	0.313	−0.079	0.999	0.307	−0.063	0.992	0.320	−0.081	0.992
	2	0.632	−0.160	0.999	0.632	−0.215	0.999	0.605	−0.174	0.991	0.637	−0.217	0.994
	3	0.929	−0.303	0.999	0.937	−0.383	0.999	0.893	−0.328	0.992	0.956	−0.392	0.995

We have been pleased to find as well that similar results are obtained using other population analysis strategies: the results for the AIM and APT changes shown in the Supporting Information (for the MP2(full)/6-311+G* model chemistry) conform qualitatively to what we observe for the NBO results, with $R^2 \geq 0.94$.[38] Even though the a and b parameters in Table 2 are method specific, the linear correlations are uniformly high.

3.4.2. Sensitivity of q_M to X, and Neutral Substitutions. Figure 4a,b and Table 2 are instructive; the transient nature of the M-neutral substitution effect is demonstrated for all the group 14 elements. It is clear from the Δq data in Figure 4a,b, for example, that $\Delta q_M = 0$ (the horizontal axes in those graphs) is approached or intersected for all five of the M centers. The actual halide for which this neutral substitution point is achieved (along the way from X = Cl to X = I) varies depending on the identity of M. As M gets larger, more polarizable, and more sensitive to the polarizing power of substituents, the point at which the neutral substitutions are observed moves from X = Cl toward X = I. In Figure 4a,b, for example, $\Delta q_M \approx 0$ for X = Br for M = C, Si, and Ge, but the neutral saturation effect is best observed at X = I for M = Sn and Pb.

3.4.3. Additional Implications of the Relationship $\Delta q_M = a(\Delta\chi_{(A'-A)}) + b$. Equation 4 emerged heuristically for us out of an effort to understand neutral substitutions and the saturation phenomenon. A rigorous derivation of the relationship between Δq_M and $\Delta\chi_{(X-H)}$ (such as the search for a universal equation that accounts for the dependence of a and b on the polarizability of M, for example) has not been attempted in this work. However, the generally very high correlation coefficients in Table 2 suggest that the linear relationships predicted by eq 4 persist across several different model chemistries so that, if we know Δq_M for any two of the halide atoms at a given level of theory, we can predict how the central atom will be affected if we opt for some other X substituent. The results in Figure 4a,b also provide insights into the different influences of one halogen substitution vs another (such as the opposing effects of F vs I substitutions) on the charge density at M.

We consider, however, that Figure 4a,b provides only a soft test for the general equation $\Delta q_M = a(\Delta\chi_{(A'-A)}) + b$; that is, because χ_H is common to all the points plotted in each line in Figure 4a,b we could treat χ_H as a constant in eq 4 and simply plot $\Delta q_{M(n\to n')}$ vs χ_X. A far more demanding test, therefore, is one in which A and A′ are different halogen substituents (with n X′ atoms substituted for n X atoms in $MH_{4-n}X_n$). In that case, if we consider all six possible pairwise (X′ ↔ X) combinations of the four halides, there is no single χ_X common to all the data points.

We find that even for X′ ↔ X substitutions, eq 4 is a very good fit (Figure 5). We hardly observed any instance of an M-neutral substitution (i.e., $\Delta q_{M(n\to n')} = 0$) in Figure 5 because, by eq 4, the incoming X′ and leaving X groups have very different electronegativities. We get close, however, for the nBr ↔ nI and nCl ↔ nBr substitutions, where the differences between the X and X′ electronegativities are smallest.

We have been satisfied to find this much more general validation of eq 4. Nonetheless, we must caution that (i) eq 4 is not perfect; there are slight but systematic deviations of the F ↔ X vs the Cl ↔ X and Br ↔ X data points for each of the n = 1 through to the n = 4 lines in Figure 5. Moreover, (ii) the particular equations that hold for the halogens in Figure 5 cannot be extended to other substituents with significantly different valence shell structures or modes of bonding to M. Even the equations for A = H, for example, which we discussed earlier in this work (Figure 4a,b) follow different linear trajectories compared to the cases where A is a halide (Figure 5). That the charge transfers for each of the nX′ ↔ nX halide substitutions follow a single unifying equation in Figure 5 is remarkable, but the function is specific to the group 17 halogen substituents.

The observed linear relationships between combinations of halogen substitutions provide a reliable index for anticipating the influence of various substitutions (of one halide by another) on the polarities and reactivities of haloalkanes (and their heavy analogues). Further work will be necessary, however, to test the validity of these linear relationships between Δq_M and $\Delta\chi_{(X-H)}$ for larger halogenated organic and inorganic molecules.

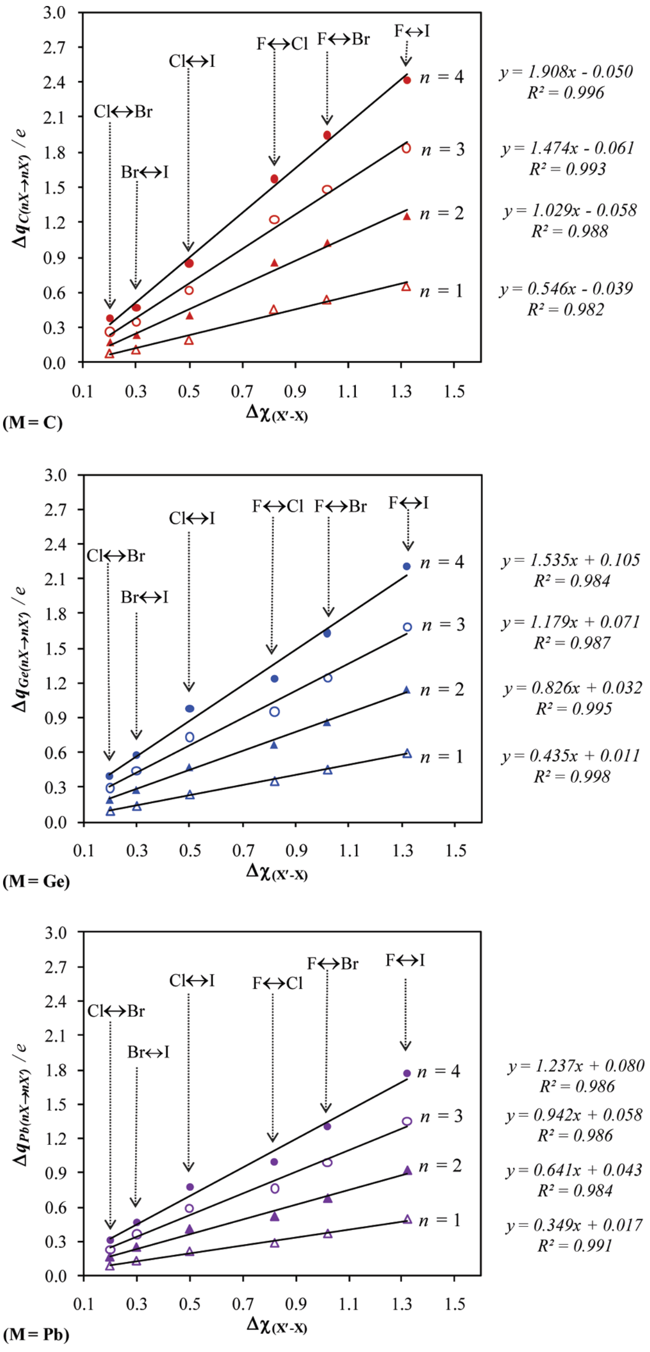

Figure 5. $\Delta q_{M(nX\rightarrow nX')}$ vs $\Delta\chi_{(X'-X)}$ going from $MH_{4-n}X_n$ to $MH_{4-n}X'_n$ for M = C, Ge, and Pb for the CCSD/aug-cc-pVTZ (NBO) q_M data. (M = Si, and Sn are included in the Supporting Information.)

3.4.4. Beyond the Teflon Limit: X Saturation in the Halogenated Inorganic Compounds. Broadly defined, "charge saturation" refers to the attainment of an optimal electron density by an atom in a molecule such that the charge at that atomic site is insensitive to significant perturbations to its bonding environment. The concept is relevant, to both central and terminal atoms, but it is probably best applied to negatively charged terminal atoms. As we have seen for the central atom in the $MH_{4-n}X_n$ molecules, what we identified initially as a saturation at M is a fortuitous instance in which the charge at M is nearly the same before and after the substitution. This phenomenon is now described, therefore, as a "neutral substitution" (of H by Br in the bromomethanes, for instance) rather than an instance of actual saturation.

The situation is completely different for terminal atoms, however. We have identified what appear to be very clear instances of terminal atom saturation in the $MH_{4-n}F_n$ systems for M ≠ C. We anticipated fluorine saturation for the case where M = C, consistent with the observations of Wiberg et al. for fluoroalkanes.[11,14,16] That essentially n-independent q_F in the halomethanes is, in fact, what we describe in the title of this section as the "Teflon limit": a constant C → F charge transfer that is quite insensitive to the bonding environment of C. We find, however, that q_F is significantly more negative for the heavier $MH_{4-n}X_n$ systems (where M ≠ C) compared to the so-called Teflon limit and is surprisingly independent of both n and M.

For an especially transparent illustration of this observation, we recast in Figure 6 the data presented initially in Figure 1b. The charges at F in all the inorganic $MH_{4-n}F_n$ systems are roughly independent of n (satisfying our basic criterion for saturation) and are remarkably independent of M as well (especially for $n = 2$, 3, and 4; see the X = F case for M ≠ C in Figure 6).

To be sure, q_F for M = C (see the red dots for X = F in Figure 6) hardly changes as a function of n. This is the well-known F-saturation in fluoromethanes, but it appears to be a nonoptimal saturation compared to the M-transferable q_F values for the Si, Ge, Sn, and Pb fluorides. The lower (but also very constant) F charges in the halomethanes may be explained by (i) the severe constraints within the carbon hybrid orbitals on how much charge density is transferable to F from C given the very low polarizability of C[39] and (ii) a minimization the F---F Coulomb repulsion, which (along with the C---F attraction) intensifies as q_F increases.[12] It seems, therefore, that the special size and electronic effects for which carbon (indeed, all of period two) is famous forces F to settle for less, far short of a full saturation, when M = C.

The n and M transferability of the F charges for M ≠ C is clear from Figure 6. The other halides appear to approach saturation regimes of their own as well, although their q_{Cl}, q_{Br}, and q_I charges span a somewhat wider range than do the q_F values. This larger variation in q_X for X = Cl, Br, and I has, of course, been explained previously; those less polarizing (less electronegative) substituents are inherently less able to maintain their charge density and are inherently more vulnerable to perturbations to their electronic environment (be it a change in n or M). To sum up, substituent saturation becomes increasingly possible as the central atom becomes more polarizable. It occurs easiest for the most polarizing substituents (F in this case) and is a fundamentally different phenomenon from the coincidental net "neutral substitutions" that cause the charge at M in $MH_{4-n}X_n$ to remain nearly constant for all n values for certain X substituents. For terminal atoms, charge saturation is a convergent phenomenon that is realizable when the electron withdrawing power of the terminal atom is satisfied by a sufficiently soft M center.

4. SUMMARY AND OUTLOOK

Using a point charge description of the bonding in $MH_{4-n}X_n$ systems (M = C, Si, Ge, Sn, Pb), we have shown that the change in the charge distribution at M, Δq_M, as n

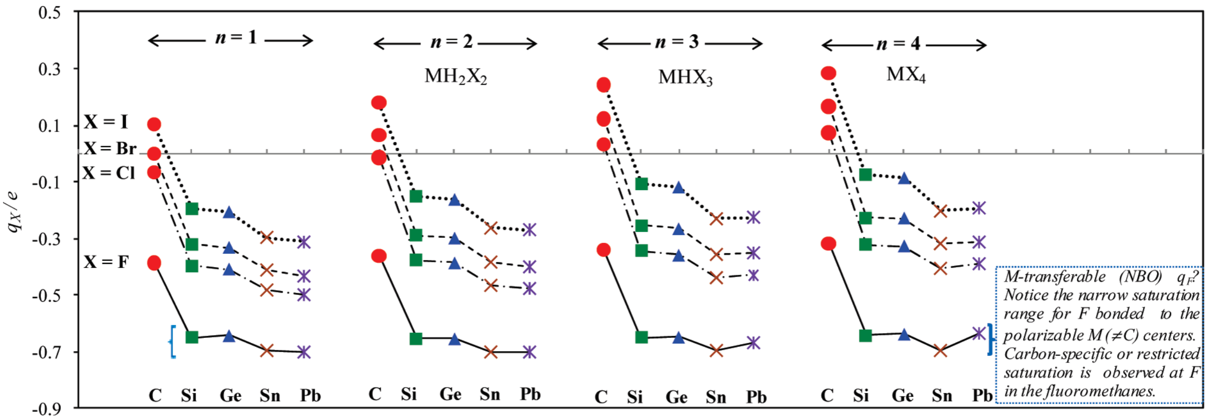

Figure 6. NBO point charges obtained at the CCSD level of theory for the halides, q_X. For the elements preceding Sn in the periodic table, the aug-cc-pVTZ basis sets were used. For the heavier elements the basis sets and ECPs are given in the Computational Methods.

increases, has a universal and strong linear correlation (for all M) with the difference in the electronegativity of H and the X substituent: that is, $\Delta q_{M(n \to n')} = a \cdot \Delta\chi_{(X-H)} + b$. This simple relationship accounts for an apparent saturation at M centers as X gets larger and exposes it as a point along a continuum; a coincidental waypoint en route from a positive Δq_M for X = F to a low or even negative Δq_M for X = I. This special case where $\Delta q_{M(n \to n')} \approx 0$ occurs in the NBO data, for example, for X = Br and M = C, but for M = Sn or Pb, it appears when X = I. Rather than saturation, we view this phenomenon as a net "neutral substitution" where a terminal atom substitution hardly modifies the charge density at the central atom (compared to the situation before the substitution).

Charge saturation is easily observed in electronegative substituents, however. A fundamental manifestation of terminal atom saturation is observed for the first time in the $MH_{4-n}F_n$ molecules for M ≠ C. The previously identified saturation at F in the organic compounds[14] appears to be a restricted C → F charge transfer that is hindered by the very low polarizability of C compared to the larger elements in group 14.[39] The lifting of this polarizability restriction, which starts at M = Si as we go down group 14, uncovers a persistent (i.e., an n and M transferable) charge saturation at the terminal fluorides. There are hints of an aspiration to saturation for the heavier halide substituents, too. The q_{Cl}, q_{Br}, and even the q_I values in Figure 6 begin to level off somewhat for M = Si to M = Pb, but those more polarizable halides are hardly capable of maintaining an n or M independent charge when compared to the fluorides.

To be sure, there are well established limitations inherent in a point charges only view of the charge distribution in molecules. Without a more detailed description of the polarization of the electron density around the nuclei, it is impossible to accurately reproduce certain measurable properties of the charge distribution such as the dipole moments. Asymmetry in the charge distribution in molecules and the differences between the position of the nuclei and the centroid of the electron density make it necessary to take higher order contributions into account. An assessment of the ability of population analysis methods to model the dipole moments of these systems is beyond the scope of this work, but a generalized representation of electron density in molecules continues to be of significant interest.

The evidence that F attains its saturation limit when M ≠ C such that $|q_{F(M \neq C)}| > |q_{F(M=C)}|$ prompts speculation about potentially significant differences in the van der Waals and electrostatic interactions with fluorinated organic solutes or surfaces coated with organic fluoropolymers[40] vs their heavier group 14 analogues. For Teflon coated materials, for instance, the hydrophobicity and coefficients of friction are strongly influenced by the charge density on F. We consider that it would be interesting to explore the influence of the magnification of the charge density at F in inorganic Teflon analogues that is implied by the data summarized in Figure 6. On that score, much more computational and experimental work remains to be done.

■ ASSOCIATED CONTENT

Ⓢ Supporting Information. Complete Gaussian 03 citation. MP2(full) and experimental geometrical data for the $MH_{4-n}X_n$ molecules and NBO point charges for M, H, and X at the various computational levels. Sample plots of the charges at M and X, Δq_M vs $\Delta\chi_{(A'-A)}$ for the NBO, APT, and AIM population analyses. This material is available free of charge via the Internet at http://pubs.acs.org.

■ AUTHOR INFORMATION

Corresponding Author

*Tel: 804-484-1628. Fax: 804-287-1897. E-mail: kdonald@richmond.edu.

■ ACKNOWLEDGMENT

This research was supported by awards from Research Corporation (Cottrell College Science Award #7742) and from the Thomas F. and Kate Miller Jeffress Memorial Trust (Award J-903). The funders mentioned above also supported the work of M.G. We thank the University of Richmond for the award of a (Chemistry Department) Puryear-Topham research fellowship to B.K.W. and Arts and Sciences research fellowships to B.K.W. and C.C. This material is based upon work supported by the National Science Foundation under (NSF-MRI) CHE-0958696 and (NSF-CAREER) CHE-1056430. We thank Kenneth Wiberg for comments, and acknowledge the reviewers for helpful suggestions.

REFERENCES

(1) (a) Sacks, L. J. *J. Chem. Educ.* **1986**, *63*, 288. (b) Gillespie, R. J. *J. Chem. Educ.* **2001**, *78*, 1688. (c) Ouyang, Y.; Ye, F.; Liang, Y. *Phys. Chem. Chem. Phys.* **2009**, *11*, 6082. (d) Chen, D.-L.; Stern, A. C.; Space, B.; Johnson, J. K. *J. Phys. Chem. A* **2010**, *114*, 10225.

(2) As an example of a more recent contribution to the discussion see: Bader, R. F. W.; Matta, C. F. *J. Phys. Chem. A* **2004**, *108*, 8385.

(3) Rittner, E. S. *J. Chem. Phys.* **1951**, *19*, 1030.

(4) (a) Parr, R. G.; Borkman, R. F. *J. Chem. Phys.* **1968**, *49*, 1055. (b) Borkman, R. F.; Simons, G.; Parr, R. G. *J. Chem. Phys.* **1969**, *50*, 58.

(5) (a) Eliezer, I. *Theor. Chim. Acta* **1970**, *18*, 77. (b) Eliezer, I.; Reger, A. *Theor. Chim. Acta* **1972**, *26*, 283. (c) Simons, G. *J. Chem. Phys.* **1972**, *56*, 4310. (d) Guido, M.; Gigli, G. *J. Chem. Phys.* **1976**, *65*, 1397.

(6) DeKock, R. L.; Peterson, M. A.; Timmer, L. K.; Baerends, E. J.; Vernooijs, P. *Polyhedron* **1990**, *9*, 1919. DeKock, R. L.; Peterson, M. A.; Timmer, L. K.; Baerends, E. J.; Vernooijs, P. Erratum. *Polyhedron* **1991**, *10*, 1965.

(7) Kaupp, M.; Schleyer, P. v. R.; Stoll, H.; Preuss, H. *J. Am. Chem. Soc.* **1991**, *113*, 6012.

(8) Donald, K. J.; Mulder, W. H.; Szentpály, L. v. *J. Chem. Phys.* **2003**, *119*, 5423.

(9) (a) Szentpály, L. v.; Gardner, D. O. N. *J. Phys. Chem. A* **2001**, *105*, 9467. (b) Donald, K. J.; Mulder, W. H.; Szentpály, L. v. *J. Phys. Chem. A* **2004**, *108*, 595.

(10) (a) Gasteiger, J.; Marsili, M. *Tetrahedron* **1980**, *36*, 3219. (b) The PEOE procedure described in ref 10a has been implemented for example in the PIMM program (see ref 10c). (c) Smith, A. E.; Lindner, H. J. *J. Comput. Aided Mol. Des.* **1991**, *5*, 235. (d) Duan, Y.; Wu, C.; Chowdhury, S.; Lee, M. C.; Xiong, G.; Zhang, W.; Yang, R.; Cieplak, P.; Luo, R.; Lee, T.; Caldwell, J.; Wang, J.; Kollman, P. *J. Comput. Chem.* **2003**, *24*, 1999.

(11) For a coherent description of these and several other procedures for obtaining atomic point charges see: Wiberg, K. B.; Rablen, P. R. *J. Comput. Chem.* **1993**, *14*, 1504.

(12) Donald, K. J.; Böhm, M. C.; Lindner, H. J. *J. Mol. Struct. (THEOCHEM)* **2004**, *710*, 1.

(13) Donald, K. J.; Böhm, M. C.; Lindner, H. J. *J. Mol. Struct. (THEOCHEM)* **2005**, *713*, 215.

(14) Wiberg, K. B.; Rablen, P. R. *J. Am. Chem. Soc.* **1993**, *115*, 614.

(15) Donald, K. J.; Wittmaack, B. K.; Crigger, C. *J. Phys. Chem. A* **2010**, *114*, 7213.

(16) Castejon, H. J.; Wiberg, K. B. *J. Org. Chem.* **1998**, *63*, 3937.

(17) (a) Carpenter, J. E.; Weinhold, F. *J. Mol. Struct. (THEOCHEM)* **1988**, *169*, 41. (b) Reed, A. E.; Curtiss, L. A.; Weinhold., F. *Chem. Rev.* **1988**, *88*, 899 and references therein. (c) We use the NBO program as implemented in *Gaussian 03*, revision E.01; *NBO*, Version 3.1; Glendening, E. D.; Reed, A. E.; Carpenter, J. E.; Weinhold, F.

(18) Bader, R. F. W. *Atoms in Molecules. A Quantum Theory*; Clarendon Press: Oxford, U.K., 1990.

(19) Cioslowski, J. *J. Am. Chem. Soc.* **1989**, *111*, 8333.

(20) (a) Head-Gordon, M.; Head-Gordon, T. *Chem. Phys. Lett.* **1994**, *220*, 122 and references therein. (b) The MP2(full) method takes all the (core and valence) electrons into account in the correlation calculations. Even in cases where the common abbreviation "MP2" is used in describing calculations performed in this work, it is always in reference to the "full" implementation of the method.

(21) (a) Krishnan, R.; Binkley, J. S.; Seeger, R.; Pople, J. A. *J. Chem. Phys.* **1980**, *72*, 650. (b) McLean, A. D.; Chandler, G. S. *J. Chem. Phys.* **1980**, *72*, 5639. (c) See also: Curtiss, L. A.; McGrath, M. P.; Blaudeau, J.-P.; Davis, N. E.; Binning, R. C., Jr.; Radom, L. *J. Chem. Phys.* **1995**, *103*, 6104 and references therein.

(22) (a) Metz, B.; Stoll, H.; Dolg, M. *J. Chem. Phys.* **2000**, *113*, 2563 (ECPs for Sn and Pb). (b) Peterson, K. A.; Shepler, B. C.; Figgen, D.; Stoll, H. *J. Phys. Chem. A* **2006**, *110*, 13877 (for I). (c) The correlation consistent triple-ζ (cc-pVTZ-pp) basis sets used are from the website of the Institute for Theoretical Chemistry at the University of Stuttgart: http://www.theochem.uni-stuttgart.de/pseudopotentials/clickpse.en.html. (d) Peterson, K. A. *J. Chem. Phys.* **2003**, *119*, 11099 (for Sn and Pb). (e) See ref 22b for the basis set used for I. (f) Peterson, K. A.; Figgen, D.; Goll, E.; Stoll, H.; Dolg, M. *J. Chem. Phys.* **2003**, *119*, 11113 (ECP and basis set for At).

(23) The 6-311+G* basis set (ref 21) with diffuse and (p) polarization functions added to H.

(24) Dunning's correlation consistent basis sets: Kendall, R. A.; Dunning, T. H., Jr.; Harrison, R. J. *J. Chem. Phys.* **1992**, *96*, 6796.

(25) (a) Here, the basis sets referenced in ref 24 are augmented by placing one s, one d, and one p diffuse function on the hydrogen atoms, and one s, one p, one d, and one f diffuse function on B through to Ne, Al through to Ar, and Sc through to Kr. (b) Woon, D. E.; Dunning, T. H., Jr. *J. Chem. Phys.* **1993**, *98*, 1358.

(26) Roothaan, C. C. J. *Rev. Mod. Phys.* **1951**, *23*, 69.

(27) (a) Burke, K.; Perdew, J. P.; Wang, Y. *Electronic Density Functional Theory: Recent Progress and New Directions*; Dobson, J. F., Vignale, G., Das, M. P., Eds.; Springer: New York, 1998. (b) Perdew, J. P.; Burke, K.; Wang, Y. *Phys. Rev. B* **1996**, *54*, 16533 and references therein.

(28) (a) Scuseria, G. E.; Janssen, C. L.; Schaefer, H. F., III. *J. Chem. Phys.* **1988**, *89*, 7382. (b) Scuseria, G. E.; Schaefer, H. F., III. *J. Chem. Phys.* **1989**, *90*, 3700.

(29) Frisch, M. J. et al. *Gaussian 03*, Revision E.01; Gaussian, Inc.: Pittsburgh, PA, 2003 (complete citation in Supporting Information).

(30) Compare Figure 1a,b in this work and Figure 3a,b in ref 15. In ref 15, the set of charges obtained at the MP2/6-311+G* level were discussed as part of a larger study of halogen bonding. The pseudopotentials described in the Computational Methods in this work were also used in ref 15 for the elements heavier than Br.

(31) The rehybridization at stage ii is accompanied by small changes in the geometry of the molecule. These modifications in the bond angles and distances have been chronicled in refs 13 and 15. In the scheme in Figure 2, they are assumed to occur at stage iii when the structure relaxes, even though we do not illustrate or specifically consider that structural aspect in this work.

(32) (a) Bratsch, S. G. *J. Chem. Educ.* **1988**, *65*, 34. (b) Bratsch, S. G. *J. Chem. Educ.* **1988**, *65*, 223.

(33) For the most electronegative X atom, F, the back-flow at stage 3, Δq_F, is small relative to q_F before the substitution. However, Δq_I can be a quite significant relative to the already small q_I (see the point charge date in the Supporting Information).

(34) Emsley, J. *The Elements*, 3rd ed.; Oxford University Press: Oxford, U.K., 1998.

(35) An easy way to confirm that the Mulliken χ_X values will show a similar relationship to Δq_M is to actually show by plots of χ_P vs χ_M (ground and valence state) that all three sets of electronegativities are linearly related to each other.

(36) Pauling, L. *Nature of the Chemical Bond*; 3rd ed.; Cornell University Press: Ithaca, NY, 1960; pp 88−95.

(37) The evident connection between Δq_M (when H is replaced by X) and the H—X bond dissociation energy is reasonable. The atom that cause the greatest charge shift in the M—X bond (relative to the charge shift in M—H bonds) is expected to form the strongest H—X bond, precisely because it will have the largest charge shift in the H—X bond as well. The H—F bond dissociation energy is high (compared to the dissociation energies for the H—Cl, H—Br, and H—I bonds) for precisely that reason.

(38) For the AIM population analyses, we consider only the C, Si, and Ge, compounds with X = F, Cl, and Br. The AIM population analysis method was not available for systems with atoms heavier than Br because, for those elements, we did not employ all electron basis sets. Both the AIM and the APT charges are reported for the MP2/6-311+G* model chemistry. Vibrational analyses, which are prerequisites for the APT calculations, are valid only for structures optimized at the same (MP2/6-311+G*) level as that used for the vibrational analysis.

(39) *CRC Handbook of Chemistry and Physics*, 91st ed. (Internet Version); Haynes, W. M., Ed.; CRC Press/Taylor and Francis: Boca Raton, Fl, 2010−2011; pp 10-186 to 10-188. The average ground state static electric dipole polarizabilities of the group 14 elements are 1.67, 5.53, 5.84, 7.84, and 7.01 Å^3, for C, Si, Ge, Sn, and Pb, respectively.

(40) Dalvi, V. H.; Rossky, P. J. *Proc. Natl. Acad. Sci. U. S. A.* **2010**, *107*, 13603.